Dual Nature of Magnetism in a Uranium Heavy-Fermion System

Jooseop Lee,[1,2,*] Masaaki Matsuda,[3] John A. Mydosh,[4] Igor Zaliznyak,[5] Alexander I. Kolesnikov,[3] Stefan Süllow,[6] Jacob P. C. Ruff,[1] and Garrett E. Granroth[3]
[1]CHESS, Cornell University, Ithaca, New York 14853, USA
[2]CALDES, Institute for Basic Science, Pohang 37673, Korea
[3]Neutron Scattering Division, Oak Ridge National Laboratory (ORNL), Oak Ridge, Tennessee 37831, USA
[4]Kamerlingh Onnes Laboratory and Lorentz Institute, Leiden University, 2300 RA Leiden, Netherlands
[5]CMPMSD, Brookhaven National Laboratory, Upton, New York 11973, USA
[6]Technische Universität Braunschweig, Braunschweig, Germany

(Received 5 October 2017; published 30 July 2018)

The duality between the localized and itinerant nature of magnetism in $5f$-electron systems has been a long-standing puzzle. Here, we report inelastic neutron scattering measurements, which reveal both local and itinerant aspects of magnetism in a single-crystalline system of UPt_2Si_2. In the antiferromagnetic state, we observe a broad continuum of diffuse magnetic scattering with a resonancelike gap of ≈ 7 meV and the surprising absence of coherent spin waves, suggestive of itinerant magnetism. While the gap closes above the Néel temperature, strong dynamic spin correlations persist to a high temperature. Nevertheless, the size and temperature dependence of the total magnetic spectral weight can be well described by a local moment with $J = 4$. Furthermore, polarized neutron measurements reveal that the magnetic fluctuations are mostly transverse, with little or none of the longitudinal component expected for itinerant moments. These results suggest that a dual description of local and itinerant magnetism is required to understand UPt_2Si_2 and, by extension, other $5f$ systems, in general.

DOI: 10.1103/PhysRevLett.121.057201

The degree of localization of magnetic moments is an important concept for understanding many exotic phenomena in condensed matter, thereby creating the "duality" problem [1]. The situation is even more complex in multiband electronic systems, where the localization can be orbital selective. For example, the magnetism in iron-based superconductors has been long discussed in terms of either itinerant or local-moment-only models. Recent progress in this field, however, suggests that this system belongs to the intermediate coupling region with $U/W \approx 1$ (U is the Coulomb repulsion, W the bandwidth), where we do not have a good understanding yet even for a single band [2].

Ternary intermetallic uranium compounds UT_2M_2 (T is a transition metal, and M is Si or Ge) have been of great interest in strongly correlated electron physics during the past decades. URu_2Si_2 has a very small magnetic moment and shows the famous, yet-to-be-understood, phenomena of hidden order and unconventional superconductivity [3]. UPt_2Si_2, on the other hand, has been long considered a rare example of a uranium intermetallic compound with strongly localized f electrons. It orders antiferromagnetically ($T_N = 32$ K) along the c axis with a magnetic moment of $\approx 2\mu_B/U$ [4]. Early studies suggested that magnetic anisotropy and high field magnetization, as well as the temperature dependence of magnetic susceptibility, can be well described within a local-moment crystal electric field model [5,6].

Recent high field studies [7,8], however, question the degree of localization in this system, suggesting that the observed phase transitions under an applied magnetic field can be understood as Lifshitz transitions, an abrupt change in the topology of a Fermi surface. This view is further supported by the density functional theory (DFT) [9], which indicates that $5f$ electrons in the UPt_2Si_2 system are orbitally polarized and mostly itinerant, with only a slight tendency toward localization.

In order to understand the magnetism, specifically the interplay between the local and itinerant nature of the moments in this system, it is crucial to study the spin dynamics. However, magnetic excitations in UPt_2Si_2 have not been observed, despite the large ordered magnetic moment. An early inelastic neutron scattering study [10] provided very limited information (at 77 K) due to the polycrystalline nature of the sample, while a more recent work [11] did not find any spin waves below ~ 3 meV.

Here, we present comprehensive neutron inelastic scattering results demonstrating that both the itinerant and local-moment nature of f electrons are playing a role in this system. We observe a diffuse magnetic excitation continuum with a resonancelike gap of ≈ 7 meV, which clearly cannot be explained by the spin wave theory for coherent collective excitation of localized moments. Rather, the excitation can be understood within the random-phase approximation (RPA) model response of the itinerant system.

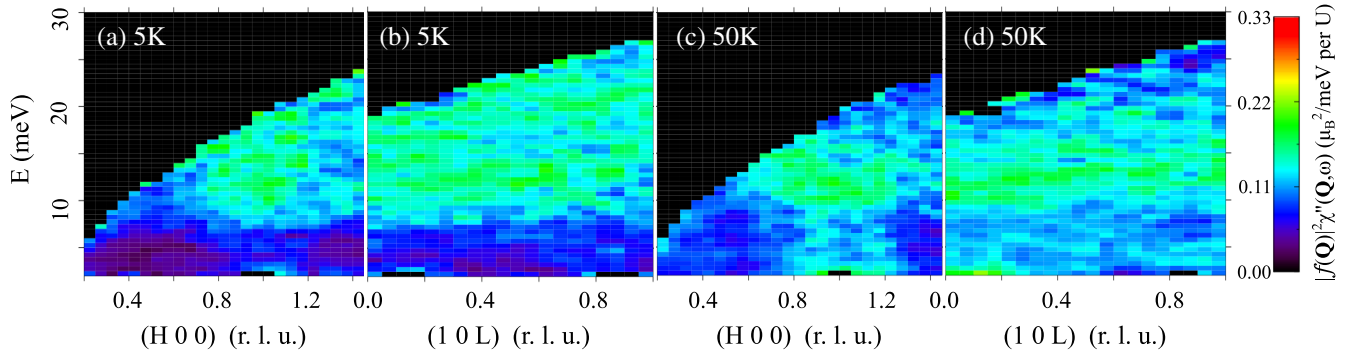

FIG. 1. The imaginary part of the dynamical magnetic susceptibility, $\chi''(\mathbf{Q},\omega)$, corrected for the U^{4+} magnetic form factor, at 5 [(a), (b)] and 50 K [(c),(d)]. The measurement was performed at SEQUOIA, with incident energy $E_i = 50$ meV.

The size and temperature dependence of the total magnetic moment, however, can be well described by a local model with $J = 4$, a total angular momentum associated with a local magnetic moment, $\hat{\boldsymbol{\mu}} = g\mu_B\hat{\mathbf{J}}$. Polarized neutron measurements also reveal that the fluctuations are mostly transverse to the staggered ordered moment. While an ordered local moment produces a transverse fluctuation, an itinerant moment also has longitudinal dynamics corresponding to the fluctuation of the size of the magnetic moment [1]. These observations show that even in this large magnetic moment system a dual approach based on an itinerant and local description is necessary to fully capture its nature. The duality of magnetism was also suggested in other heavy-fermion superconductors [12] and thus seems to be universal across $5f$-electron systems.

All measurements presented here were performed on a 1.5 g single-crystalline sample of UPt_2Si_2 [13]. Initial neutron scattering measurements were done with the HB1 thermal triple axis spectrometer at the high-flux-isotope reactor, ORNL. A large volume of energy-momentum space was then explored using the time-of-flight (TOF) spectrometer SEQUOIA [16,17] at spallation neutron source, ORNL [18] with incident energies (E_i) of 50 and 100 meV. TOF neutron data were normalized to the absolute scattering cross section in $\mu_B^2/\mathrm{meV}/U$ by using a standard vanadium sample [19]. The measured scattering intensities were converted to the imaginary part of the dynamical magnetic susceptibility via the fluctuation-dissipation theorem, $\chi''(\mathbf{Q},\omega) = \pi(1-e^{-E/k_BT})S(\mathbf{Q},\omega)$ [20].

Contrary to what is expected for conventional magnetic order, a broad continuum of magnetic excitations is observed around the magnetic wave vector, $\mathbf{Q}_M = (100)$ (Fig. 1). In the local magnetism approach, interactions between local moments are described by a spin exchange Hamiltonian. The low-energy collective transverse fluctuations of ordered magnetic moments, i.e., spin waves, are expected to have well-defined sharp dispersion relations demonstrating long-range coherence. In an itinerant moment system, on the other hand, the excitations originate from electron-hole pairs created across the Fermi surface. These excitations are usually broad in Q-E space and weak in intensity, without clear dispersion.

Figures 1(a) and 1(b) present the generalized susceptibility as a function of the wave vector along the $(H\,0\,0)$ and $(1\,0\,L)$ direction, respectively, at $T \ll T_N$. The excitation is diffuse, centered around $E \approx 13$ meV, with a gap of $\approx$7 meV. The intensity in the H direction is peaked near $\mathbf{Q}_M$. The excitation along the L direction [Fig. 1(b)], in contrast, is rather flat, suggesting anisotropic magnetic interactions consistent with the quasi-two-dimensional (2D) character observed in resistivity [21] and the Fermi surface [9]. A spin gap of $\sim$7 meV, which is clearly visible in Figs. 1(a) and 1(b), is roughly consistent with the gap of 46 K estimated from the temperature dependence of resistivity [21]. Above the Néel temperature, at 50 K, this gap is closed, as shown in Figs. 1(c) and 1(d). It should be noted that spin fluctuations along $(H\,0\,0)$ are still clearly peaked around $\mathbf{Q}_M$, indicating a strong magnetic correlation even in the paramagnetic regime above T_N. We refer to Supplemental Material for more temperature dependence data [22].

As the observed excitation continuum cannot be described by the spin wave theory, we fit the data using the dynamical magnetic susceptibility calculated using the random phase approximation (RPA) in an itinerant electron model. The resulting expression is essentially identical to the extended self-consistent renormalization (SCR) theory model [1,23,24], which takes account, in a self-consistent way, of the effect of the spin fluctuation mode coupling [25]. The resulting RPA SCR expression for the generalized magnetic susceptibility is

$$\chi''(\mathbf{Q}+\mathbf{q},\omega) = \frac{\chi_Q}{1+(q/\kappa)^2}\frac{\hbar\omega\Gamma(q,\kappa)}{(\hbar\omega)^2+\Gamma(q,\kappa)^2}, \quad (1)$$

with the Q-dependent relaxation rate

$$\Gamma(q,\kappa) = \gamma_A(\kappa^2+q^2). \quad (2)$$

Parameters κ, γ_A, and χ_Q are a characteristic width in reciprocal space, a temperature-insensitive energy width

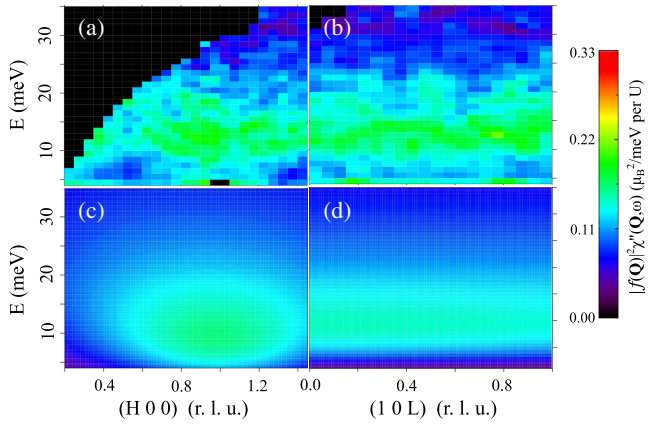

FIG. 2. (a), (b) $\chi''(\mathbf{Q},\omega)$ observed at 50 K with $E_i = 100$ meV along the H and L direction, respectively. (c), (d) Fit to the SCR or, equivalently, RPA theoretical model.

parameter, and a static staggered susceptibility, respectively. The wave vector q is measured away from $\mathbf{Q}_M$.

It is clear from Fig. 2 that Eq. (1) provides an adequate description of the observed magnetic excitation. While data with $E_i = 50$ meV reveal the 7 meV gap with better resolution, $E_i = 100$ meV data capture the full range of magnetic excitation and, therefore, were used for the global fitting. The results of the fit along the H and L directions are shown in Figs. 2(c) and 2(d). Table I lists the best fit parameters when the magnetic form factor is corefined [26,27]. The top of the excitation band is around 25 meV. The single intensity lobe is inconsistent with dispersive magnetic excitations. This demonstrates that the spin fluctuation is rather a resonance localized in Q-E space, similar to the resonance magnetic excitation observed in many unconventional superconductors such as cuprates [31], Fe-based superconductors [2], or heavy-fermion superconductors [32].

Figure 3 shows the change in the scattering intensity with a varying temperature. There is an increase of quasielastic paramagnetic scattering with the increasing temperature across T_N. The change of the spectral gap follows the order parameter dependence of magnetic Bragg peaks [4], which strongly supports the magnetic nature of fluctuations [33].

The spectral weight filling in the gap comes from other energy transfers [Fig. 3(b)]. It is clear, however, from Figs. 1 and 3, that this redistribution affects only a moderately small fraction of the total magnetic spectral weight. In this case, the ordered magnetic moment in the antiferromagnetic state, which is only $2\mu_B$, is weak and comprises only a small fraction of the fluctuating magnetic moment. Consequently, its influence on magnetic excitations is small and limited to low energies, $\lesssim k_B T_N$, which again emphasizes that the system cannot be simply understood from its ordered moment [34].

In the local-moment model, the integral spectral weight measured by neutron scattering obeys the zero-moment sum rule [20], $\sum_\alpha \int_{-\infty}^{+\infty} \int_{\mathrm{BZ}} S^{\alpha\alpha}(\mathbf{q},\omega) d\mathbf{q} dE / \int_{\mathrm{BZ}} d\mathbf{q} = (g\mu_B)^2 J(J+1)$, where α is the polarization of magnetic fluctuation, g is the spectroscopic Landé g factor, and μ_B is the Bohr magneton. By assuming random polarization of the magnetic fluctuation with respect to the wave vector transfer, which is a good approximation for the TOF data in Fig. 3(b), and fitting the Q-integrated normalized magnetic intensity [35] $S(E)$ to a model function consisting of the quasielastic Lorentzian and the damped harmonic oscillator, we obtain the integral magnetic scattering intensity of $\approx 15.9\mu_B^2$ at 5 K and $\approx 13.6\mu_B^2$ at 50 K. Using $g = 0.8$, which is appropriate for the $^3H_4$ Hund rule Russell-Saunders ground state of U^{4+} [36], this results in an estimated $J \approx 4.5$ at 5 K and ≈ 4.1 at 50 K, consistent with the $J = 4$ state. This exhausts the full magnetic spectral weight available for the $5f^2$-electronic configuration of U^{4+}, and, therefore, temperature enhancement of the integral spectral weight from the

TABLE I. Parameters obtained by fitting $E_i = 100$ meV and $T = 50$ K data with Eq. (1).

	κ(Å^{-1})	γ_A (meV/Å^{-2})	χ_Q (μ_B^2/meV)
(H 0 0)	1.35(8)	5.18(54)	0.33(1)
(1 0 L)	2.77(114)	1.21(98)	0.30(1)

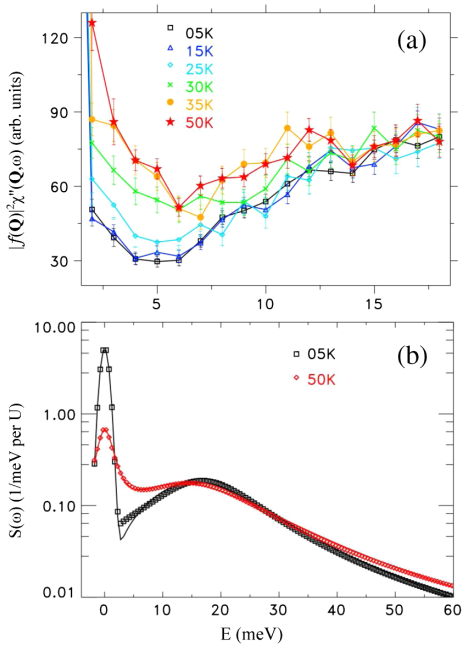

FIG. 3. Evolution of the generalized susceptibility across T_N. (a) The detailed temperature dependence of low-energy spin excitation at $\mathbf{Q} = (1,0,0)$ measured using the HB1 triple axis spectrometer. The counting time for each data point was about 5 min. (b) The autocorrelation function $S(E)$ at 5 (black square) and 50 K (red diamond), obtained from the Q-integrated spectral weight of the TOF data. Solid lines show a fit to a model function consisting of a Lorentzian centered at $E = 0$ (quasielastic) and a damped harmonic oscillator (inelastic).

TABLE II. Nuclear and magnetic components contributing to the scattering intensity at $(H\,0\,0)$ in the present polarized neutron measurement. P_n is the neutron spin polarization direction, N denotes nuclear components, and $B_{1,2}$ represent the background in the SF and NSF configuration, respectively. S_a cannot be observed in this setup, because the magnetic component parallel to $\mathbf{Q}$ does not contribute to neutron scattering.

	HF ($\mathbf{P}_n \| a$)	VF ($\mathbf{P}_n \| b$)
SF	$S_b^2 + S_c^2 + B_1$	$S_c^2 + B_1$
NSF	$N^2 + B_2$	$S_b^2 + N^2 + B_2$

entanglement between local and itinerant electrons [37] is not observed.

The integral intensity of the magnetic excitation spectrum thus indicates participation of two $5f$ electrons, as in the $J = 4$ state of U^{4+} in the local-moment picture. In order to rationalize the observed magnetic spectral weight in the itinerant-electron model of Eq. (1), one needs to recall that the approximation adopted in deriving this result [1,23,24] limits its applicability to the proximity of the Fermi energy. Hence, the integration of the spectral weight must be limited by a finite-energy cutoff Λ, which is of the order of the itinerant-electron bandwidth (otherwise, the integral formally diverges). On account of this cutoff, the total magnetic spectral weight is $\int_{-\infty}^{+\infty} \int_{\mathrm{BZ}} \chi''(\mathbf{q},\omega) d\mathbf{q} dE / \int_{\mathrm{BZ}} d\mathbf{q} \approx \chi_Q(\gamma_A \kappa^2) \ln[(\Lambda/\gamma_A\kappa^2)]$ [38]. Using the fit results from Table I, we estimate the itinerant-electron bandwidth of 1–2 eV, in good agreement with the extent of spin-polarized $5f$ bands in recent DFT calculations [8,9]. Hence, UPt_2Si_2 cannot be simply viewed as a narrow-band system where the local-moment picture applies. The observed magnetic dynamics inside the energy window probed in the present experiment is distinct from that of local moments and is well described by the RPA itinerant-electron theory. On the other hand, applying the first moment sum rule to the measured intensity and assuming the local-moment model with nearest neighbor exchange interactions, we obtain a much lower energy scale, ≈10 meV, for the contribution of magnetic bond energies per U to the ground state, consistent with the observed excitation spectrum [39].

In order to further elucidate the magnetic nature of the observed diffuse and weak excitation, we carried out a polarized neutron measurement. Table II summarizes different contributions to the spin-flip (SF) and non-spin-flip (NSF) intensities when the scattering plane is $(H\,0\,L)$ and the neutron spin is parallel to either the a-axis (HF denotes horizontal field) or the b-axis (VF denotes vertical field) directions. Since U magnetic moments are aligned along the c axis, $S_{a,b}$ corresponds to transverse fluctuations while S_c indicates a longitudinal fluctuation.

Figure 4 presents polarized neutron scans below T_N at constant $E = 12$ meV along the $(H\,0\,0)$ direction, which reveal a small but clear magnetic signal whose Q dependence is consistent with that observed with unpolarized

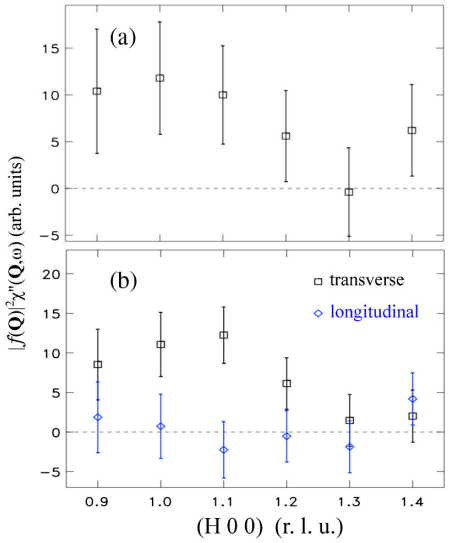

FIG. 4. Polarized neutron measurement at constant $E = 12$ meV at $T = 5$ K. (a) Magnetic scattering (= HF-SF − HF-NSF in Table II). (b) Transverse spin fluctuation S_b (= HF-SF − VF-SF or VF-NSF − HF-NSF) and estimated longitudinal spin fluctuation S_c (= HF-SF − VF-NSF or VF-SF − HF-NSF). Each data point has been counted for about 3 hr.

neutrons (Fig. 2). The polarization of magnetic fluctuation can be further analyzed by comparing different scattering setups. The intensity difference between HF and VF configurations, in either the SF or NSF, directly yields S_b, the transverse fluctuation. Black squares in Fig. 4(b) show the transverse fluctuation. The longitudinal component can be evaluated from the difference of HF-SF and VF-NSF (or VF-SF and HF-NSF) assuming that $N^2 + B_2$ and B_1 do not differ, which is valid since the total magnetic signal [Fig. 4(a)] corresponds to the sum of transverse and longitudinal signals [Fig. 4(b)]. The estimated longitudinal fluctuation shown as blue diamond symbols in Fig. 4(b) appears to have negligible intensity. This indicates that spin fluctuations are primarily transverse, in sharp contrast with the longitudinal magnetic dynamics observed in chromium, the archetypal example of an itinerant antiferromagnet [41], and in other uranium compounds such as UN [42] and URu_2Si_2 [43].

Our comprehensive inelastic neutron scattering studies thus show that itinerant electrons are playing a major role in the dynamical magnetism of UPt_2Si_2. Despite the large ordered magnetic moment revealed by neutron diffraction [4], the magnetic excitations are broad and resonancelike, lacking a sharp dispersion, and could be understood in the itinerant RPA approach. Above T_N, the gap in the excitation spectrum is closed, but the strong magnetic correlation is still present. The temperature dependence of spectral weight shows that only a small fraction of magnetic excitation changes across the Néel temperature, and the system should not be described solely from its ordered moment.

Our results make it clear that this system is at the boundary where both local-moment and itinerant degrees of freedom are important, just like Fe-based superconductors or other strongly correlated electron systems. Many physical properties previously attributed exclusively to the local nature, e.g., field-induced phase transitions [7], could be indeed consequences of this magnetic duality. The lack of an adequate theory to comprehensively describe the observed behaviors calls for a new modeling effort with UPt_2Si_2 as a test case for duality. Considering the universal magnetic duality in $5f$-electron systems, other overlooked large moment uranium intermetallics [44–47] should also be reexamined.

We thank Guangyong Xu and T. J. Williams for helpful discussion on data analysis. This research at High Flux Isotope Reactor and Spallation Neutron Source of ORNL was sponsored by the Scientific User Facilities Division, Office of Basic Energy Sciences, U.S. Department of Energy, and the Laboratory Directors Research and Development fund of ORNL. Cornell High Energy Synchrotron Source was supported by the NSF and NIH/National Institute of General Medical Sciences via NSF Award No. DMR-1332208. The work at Brookhaven National Laboratory was supported by the Office of Basic Energy Sciences, U.S. Department of Energy, under Contract No. DE-SC0012704.

*Quantum Condensed Matter Division, Oak Ridge National Laboratory, Oak Ridge, Tennessee 37831, USA.

[1] T. Moriya, *Spin Fluctuations in Itinerant Electron Magnetism* (Springer-Verlag, Berlin, 1985).
[2] P. Dai, J. Hu, and E. Dagotto, Nat. Phys. **8**, 709 (2012).
[3] J. A. Mydosh and P. M. Oppeneer, Rev. Mod. Phys. **83**, 1301 (2011), and references therein.
[4] R. A. Steeman, E. Frikkee, S. A. M. Mentink, A. A. Menovsky, G. J. Nieuwenhuys, and J. A. Mydosh, J. Phys. Condens. Matter **2**, 4059 (1990).
[5] G. J. Nieuwenhuys, Phys. Rev. B **35**, 5260 (1987).
[6] H. Amitsuka, T. Sakakibara, K. Sugiyama, T. Ikeda, Y. Miyako, M. Date, and A. Yamagishi, Physica B (Amsterdam) **177**, 173 (1992).
[7] D. S. Grachtrup, M. Bleckmann, B. Willenberg, S. Süllow, M. Bartkowiak, Y. Skourski, H. Rakoto, I. Sheikin, and J. A. Mydosh, Phys. Rev. B **85**, 054410 (2012).
[8] D. S. Grachtrup, N. Steinki, S. Süllow, Z. Cakir, G. Zwicknagl, Y. Krupko, I. Sheikin, M. Jaime, and J. A. Mydosh, Phys. Rev. B **95**, 134422 (2017).
[9] S. Elgazzar, J. Rusz, P. M. Oppeneer, and J. A. Mydosh, Phys. Rev. B **86**, 075104 (2012).
[10] R. A. Steeman, E. Frikkee, C. van Dijk, G. J. Nieuwenhuys, and A. A. Menovksy, J. Magn. Magn. Mater. **76**, 435 (1988).
[11] N. Metoki, Y. Koike, Y. Haga, N. Bernhoeft, G. H. Lander, Y. Tokiwa, and Y. Ōnuki, Acta Phys. Pol. B **34**, 979 (2003).
[12] S. Fujimori, Y. Saitoh, T. Okane, A. Fujimori, H. Yamagami, Y. Haga, E. Yamamoto, and Y. Ōnuki, Nat. Phys. **3**, 618 (2007).
[13] See Supplemental Material at http://link.aps.org/supplemental/10.1103/PhysRevLett.121.057201 for more details on the experimental setup, which includes Refs. [14,15].
[14] O. Arnold, J. C. Bilheux, J. M. Borreguero, A. Buts, S. I. Campbell, L. Chapon, M. Doucet, N. Draper, R. F. Leal, M. A. Gigg, V. E. Lynch, A. Markvardsen, D. J. Mikkelson, R. L. Mikkelson, R. Miller, K. Palmen, P. Parker, G. Passos, T. G. Perring, P. F. Peterson, S. Ren, M. A. Reuter, A. T. Savici, J. W. Taylor, R. J. Taylor, R. Tolchenov, W. Zhou, and J. Zikovsky, Nucl. Instrum. Methods Phys. Res., Sect. A **764**, 156 (2014).
[15] R. A. Ewings, A. Buts, M. D. Le, J. van Duijn, I. Bustinduy, and T. G. Perring, Nucl. Instrum. Methods Phys. Res., Sect. A **834**, 132 (2016).
[16] G. E. Granroth, D. H. Vandergriff, and S. E. Nagler, Physica B (Amsterdam) **385–386**, 1104 (2006).
[17] G. E. Granroth, A. I. Kolesnikov, T. E. Sherline, J. P. Clancy, K. A. Ross, J. P. C. Ruff, B. D. Gaulin, and S. E. Nagler, J. Phys. Conf. Ser. **251**, 012058 (2010).
[18] T. E. Mason, D. Abernathy, I. Anderson, J. Ankner, T. Egami, G. Ehlers, A. Ekkebus, G. Granroth, M. Hagen, K. Herwig, J. Hodges, C. Hoffmann, C. Horak, L. Horton, F. Klose, J. Larese, A. Mesecar, D. Myles, J. Neuefeind, M. Ohl, C. Tulk, X-L. Wang, and J. Zhao, Physica B (Amsterdam) **385**, 955 (2006).
[19] G. Xu, Z. Xu, and J. M. Tranquada, Rev. Sci. Instrum. **84**, 083906 (2013).
[20] I. A. Zaliznyak and S.-H. Lee, in *Modern Techniques for Characterizing Magnetic Materials*, edited by Y. Zhu (Springer, Heidelberg, 2005).
[21] S. Süllow, A. Otop, A. Loose, J. Klenke, O. Prokhnenko, R. Feyerherm, R. W. A. Hendrikx, J. A. Mydosh, and H. Amitsuka, J. Phys. Soc. Jpn. **77**, 024708 (2008).
[22] See Supplemental Material at http://link.aps.org/supplemental/10.1103/PhysRevLett.121.057201 for a wider range temperature dependence at different wave vectors.
[23] H. Hasegawa and T. Moriya, J. Phys. Soc. Jpn. **36**, 1542 (1974).
[24] K. Nakayama and T. Moriya, J. Phys. Soc. Jpn. **56**, 2918 (1987).
[25] W. Bao, C. Broholm, G. Aeppli, S. A. Carter, P. Dai, T. F. Rosenbaum, J. M. Honig, P. Metcalf, and S. F. Trevino, Phys. Rev. B **58**, 12727 (1998).
[26] The error bar does not include systemic errors from absolute normalization, which is typically about 20%.
[27] See Supplemental Material at http://link.aps.org/supplemental/10.1103/PhysRevLett.121.057201 for more details on the phenomenological magnetic form factor and its refinement, which includes Refs. [28–30].
[28] I. Zaliznyak, A. T. Savici, M. Lumsden, A. Tsvelik, R. Hu, and C. Petrovic, Proc. Natl. Acad. Sci. U.S.A. **112**, 10316 (2015).
[29] T. Moriya and K. Ueda, J. Phys. Soc. Jpn. **63**, 1871 (1994).
[30] W. Knafo, S. Raymond, P. Lejay, and J. Flouquet, Nat. Phys. **5**, 753 (2009).
[31] J. M. Tranquada, G. Xu, and I. A. Zaliznyak, J. Magn. Magn. Mater. **350**, 148 (2014).
[32] C. Stock, C. Broholm, J. Hudis, H. J. Kang, and C. Petrovic, Phys. Rev. Lett. **100**, 087001 (2008).

[33] E. G. Sergeicheva, S. S. Sosin, L. A. Prozorova, G. D. Gu, and I. A. Zaliznyak, Phys. Rev. B **95**, 020411(R) (2017).
[34] See Supplemental Material at http://link.aps.org/supplemental/10.1103/PhysRevLett.121.057201 for the SCR RPA analysis in the AFM phase.
[35] Since the accessible energy range around $\mathbf{Q} = (1, 0, 0)$ is limited due to kinematic restriction, we divided the Brillouin zone (BZ) into small areas whose integrated intensity is extrapolated to high-energy transfer by fitting to Lorentzian distribution. The final integrated intensity in Fig. 3(b) was estimated by summing each integrated intensity weighted by their BZ volume. $E_i = 50$ and 100 meV data have been used for low- (≤ 10 meV) and high-energy (≥ 10 meV) transfer, respectively, which were joined smoothly after absolute normalization.
[36] A. J. Freeman, J. P. Desclaux, G. H. Lander, and J. Faber, Jr., Phys. Rev. B **13**, 1168 (1976).
[37] I. A. Zaliznyak, Z. Xu, J. M. Tranquada, G. Gu, A. M. Tsvelik, and M. B. Stone, Phys. Rev. Lett. **107**, 216403 (2011).
[38] See Supplemental Material at http://link.aps.org/supplemental/10.1103/PhysRevLett.121.057201 for the estimation of the bandwidth in the itinerant-electron system.
[39] See Supplemental Material at http://link.aps.org/supplemental/10.1103/PhysRevLett.121.057201 for the bond energy from the first moment sum rule in neutron scattering, which includes Ref. [40].
[40] M. B. Stone, I. Zaliznyak, D. H. Reich, and C. Broholm, Phys. Rev. B **64**, 144405 (2001).
[41] E. Fawcett, Rev. Mod. Phys. **60**, 209 (1988).
[42] T. M. Holden, W. J. L. Buyers, E. C. Svensson, and G. H. Lander, Phys. Rev. B **30**, 114 (1984).
[43] F. Bourdarot, E. Ressouchea, R. Balloub, S. Raymonda, D. Aokia, N. Martina, L.-P. Regnaulta, V. Simonetb, M. T. Fernandez-Diazc, A. Stunaultc, V. Taufoura, and J. Flouquet, Phys. Procedia **42**, 4 (2013).
[44] H. Ptasiewicz-Bak, J. Leciejewicz, and A. Zygmunt, J. Phys. F **11**, 1225 (1981).
[45] B. Shemirani, H. Lin, M. F. Collins, C. V. Stager, J. D. Garrett, and W. J. L. Buyers, Phys. Rev. B **47**, 8672 (1993).
[46] L. Chelmicki, J. Leciejewicz, and A. Zygmunt, Solid State Commun. **48**, 177 (1983).
[47] J. Leciejewicz, L. Chelmicki, and A. Zygmunt, Solid State Commun. **41**, 167 (1982).